

Mieczysław ŻYŁA*, Marek OLSZAR*

CHANGES IN THE POROUS STRUCTURE OF MONTMORILLONITE AS A FUNCTION OF ITS ACID ACTIVATION TIME

UKD 549.623:552.52]montmorillonit: 548.7: 549.1: 539.217.1: 541.128.34: 542.946 „4”

A b s t r a c t. The paper presents the results of adsorption, densimetric and porosimetric studies of montmorillonite samples subjected to acid activation for different lengths of time. It has been found that total and meso-porosity of montmorillonite increase with activation time. Particularly wide differences have been noted in the range of mesopores. The volume of micropores changes insignificantly.

INTRODUCTION

Acid activation is the commonest method of modification of montmorillonite. It results in the progressive degradation of its structure, due to the replacement of exchangeable cations by H_3O^+ ions and the partial removal of Al^{3+} , Mg^{2+} and Fe^{3+} ions. These processes eventually lead to the complete breakdown of the octahedral sheet. The degradation of the tetrahedral sheet attended by the formation of silica gel is also possible. Studies carried out by Novak and Gregor (1969) have shown that there is a distinct relationship between the amount of cations being removed and the specific surface area. It has also been found that the increase in specific surface area enhances the decolourizing properties of montmorillonite, especially with respect to oil, up to a certain boundary value of area, whereupon these properties deteriorate rapidly.

Fijał et al. (1975) showed the effect of the structure of an adsorbate molecule on sorption properties of montmorillonite as a function of acid activation time. It has been noticed that the amount of sorbed vapours of nonpolar substances (argon, *n*-hexane) increases and simultaneously sorption properties deteriorate with respect to polar substances (water, methyl alcohol). This deterioration is accounted for by the reduction in the number of polar -OH groups connected with the octahedral sheet. Changes in the adsorption properties of acid activation products also depend on the kind of the interlayer cation of untreated montmorillonite (Bodek, Ziętkiewicz, Żyła 1983). So wide differences in sorption properties of montmorillonite with respect to nonpolar substances testify to the change in porous structure, occurring in

* Institute of Chemical Processing of Coal and Physical Chemistry of Sorbents, Academy of Mining and Metallurgy in Cracow (Kraków, al. Mickiewicza 30).

response to acid activation.

The porosity of clay minerals is determined by the size and mode of orientation of crystallites within the domains, the size and mode of filling of interlayer spaces, and the mutual arrangement of domains within the grain aggregates. Three types of pores are distinguished, depending on their radii (r). They are: macropores ($r > 30$ nm), mesopores ($1.5 < r < 30$ nm) and micropores ($r < 1.5$ nm). The dominant types of pores in montmorillonite are meso- and micropores (Stoch 1974). Porosimetric studies have shown that mesopores make up 30–70% of the total porosity. The content of micropores varies from 20 to 50% (Żyła 1972). The data of other authors indicate that the dominant pore radius is shifted to the range of microporous structure and the effective radius is 1.5–1.7 nm. Microporosity in montmorillonite is due to the random arrangement of layers, and the degree of disorder is connected with the kind of cation occupying the interlayer spaces.

The model of pore shape in montmorillonite presents considerable difficulties. The porous structure of most solids is too irregular and complex to be described accurately in geometrical terms. Generally the cylindrical shape of pores is assumed and calculations are made according to this assumption. A different model of pore shape was suggested by De Boer, who believes that fracture pores are dominant in the porous structure of montmorillonite.

EXPERIMENTAL

The aim of this paper was to determine the changes in the porous structure of montmorillonite subjected to acid activation at water boiling point for different lengths of time.

The studies were carried out on montmorillonite separated by sedimentation from bentonite from the Chmielnik deposit. Montmorillonite samples were activated for 1, 3, 4 and 10 hours at water boiling point. After filtration, they were washed with water until the reaction to chloride ions was negative, and then dried. The samples were designated as follows:

- W – untreated montmorillonite
- M-1 – sample activated for 1 hour
- M-3 – sample activated for 3 hours
- M-4 – sample activated for 4 hours
- M-10 – sample activated for 10 hours

The samples were hand-pressed into flat pellets. Since the pressure applied was small, binder was added to each sample in the amount of 1.2 g pure montmorillonite per 6 g activation product.

The pellets were subjected to measurements of argon sorption at very low relative pressures and over the whole range of pressures, as well as to densimetric and porosimetric studies.

RESULTS

Densimetric studies

To determine the total porosity of acid activation products, apparent (mercury) and true (helium) densities were determined. Prior to each measurement, the samples were outgassed to a pressure of $1.33 \cdot 10^{-3}$ Pa. The total pore volume V_c in 1 g of sample was calculated from the formula:

$$V_c = \frac{1}{d_{Hg}} - \frac{1}{d_{He}} \text{ (cm}^3\text{/g)}$$

From densimetric data the pore volume percentage of samples was calculated, using the simple relation:

$$\Sigma = \frac{d_{He} - d_{Hg}}{d_{He}}$$

The values obtained are listed in Table 1. From these data it appears that 1-hour activation causes a substantial increase in the total pore volume compared with the porosity of untreated sample. The maximum pore volume V_c has been noted for 3- and 10-hour activation. After longer activation time new structural phases are formed, which show an increase in free pore areas. The pore volume minimum has been noted for the sample activated for 4 hours. As was found earlier (Fijał et al. 1975), the minimum amount of ions passing into solution also corresponds to this sample. In a sample activated for this length of time, unextracted ions, particularly Ca^{2+} , form a sort of aggregates with the decreased value of total porosity.

Table 1

Total porosity, apparent and true density

Sample	d_{Hg} g/cm ³	d_{He} g/cm ³	Σ %	V_c cm ³ /g
W	2.092	2.619	20.10	0.096
M-1	1.573	2.738	42.50	0.270
M-3	1.049	2.946	64.40	0.614
M-4	1.132	2.454	53.86	0.476
M-10	0.848	2.479	65.80	0.775

The further increase in pore volume is associated with the formation of amorphous silica.

Adsorption studies

Argon sorption was determined on all the samples at 77 K, using sorption manostats (Ciembroniewicz, Lasoń 1972). Prior to measurements, the samples were outgassed to a pressure of $1.33 \cdot 10^{-3}$.

Fig. 1 presents argon adsorption isotherms obtained for the samples studied at $p/p_0 = 0.00-0.05$. These isotherms were used to calculate micropore volume W_0 , basing on Dubinin-Raduszkiewicz equation (Dubinin 1960). Fig. 2 shows argon adsorption isotherms over the whole range of relative pressures. From these isotherms BET areas were calculated. The desorption part of the adsorption isotherm served as a basis for calculating the total volume and surface area of mesopores and their differential distribution against radius (Figs. 3–7). The volume and surface area distribution was calculated using the second variant of Dubinin's method (Korta, Klinik 1979).

An analysis of respective curves reveals that acid activation causes the development of pores mainly in the range corresponding to pore radii from 1.5 to 6.0 nm. Samples activated for 3 or 4 hours develop pores of a radius of 2–6 nm. The sample after 10-hour activation shows the increased mesopore volume over the whole range of transitional porosity. The observed increase in mesopore volume in the direction of higher radius values is presented in Fig. 8, which is a plot of radius r vs. mesopore area increase ΔS_{mes} , calculated from the second variant of Dubinin's formula. The plot is based on the most characteristic ΔS intervals which illustrate well the changes occurring in the structure of montmorillonite. All the activation products show an increase in the surface area of mesopores up to 4 nm. This value of pore radius excee-

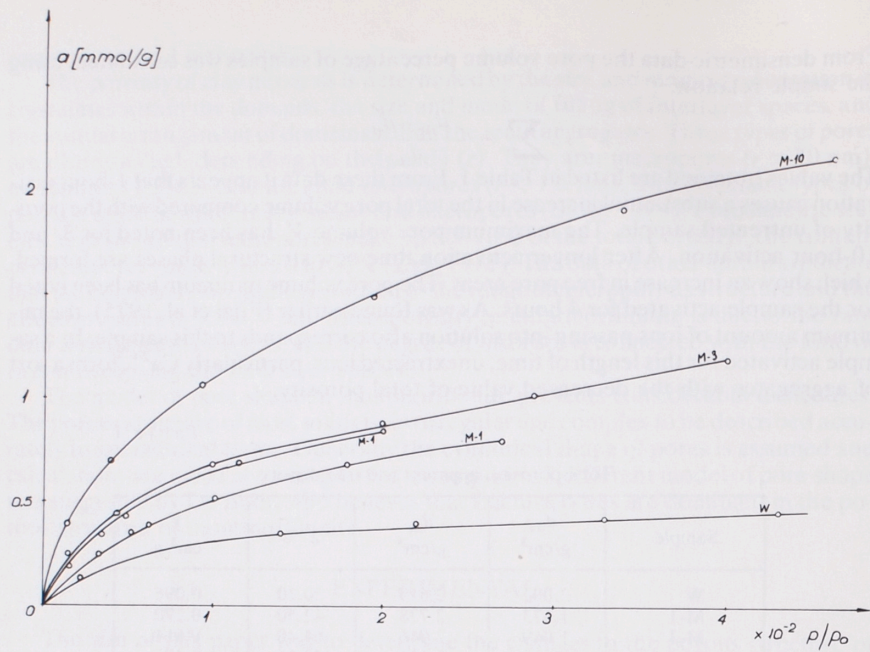


Fig. 1. Argon adsorption isotherms obtained at low relative pressures $p/p_0 = 0.00-0.05$

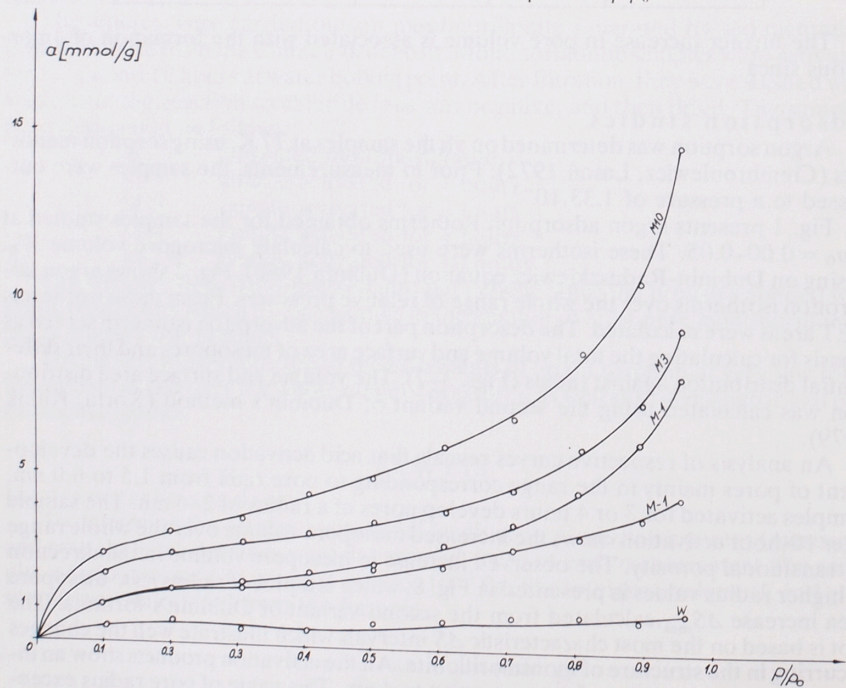


Fig. 2. Argon adsorption isotherms obtained over the whole range of relative pressures $p/p_0 = 0.05-0.97$

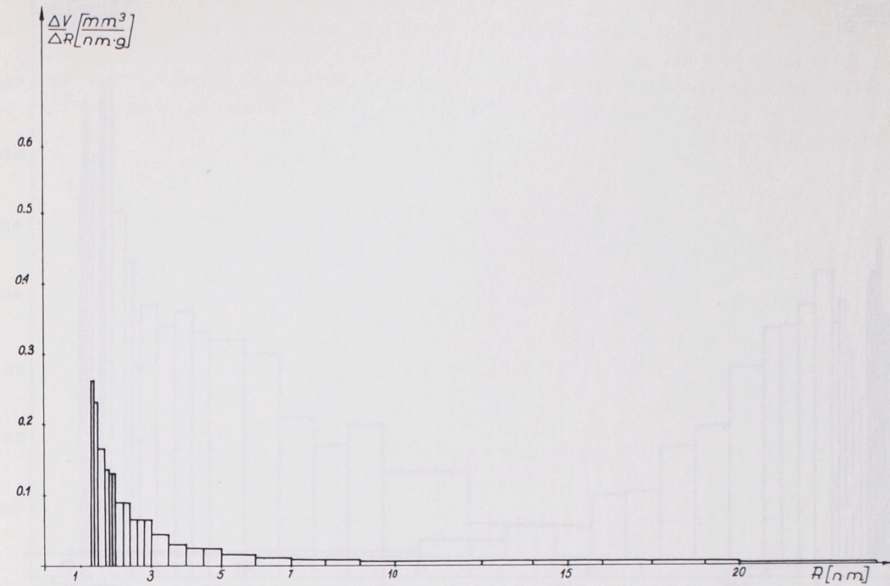


Fig. 3. Differential pore volume distribution vs. radius (sample W)

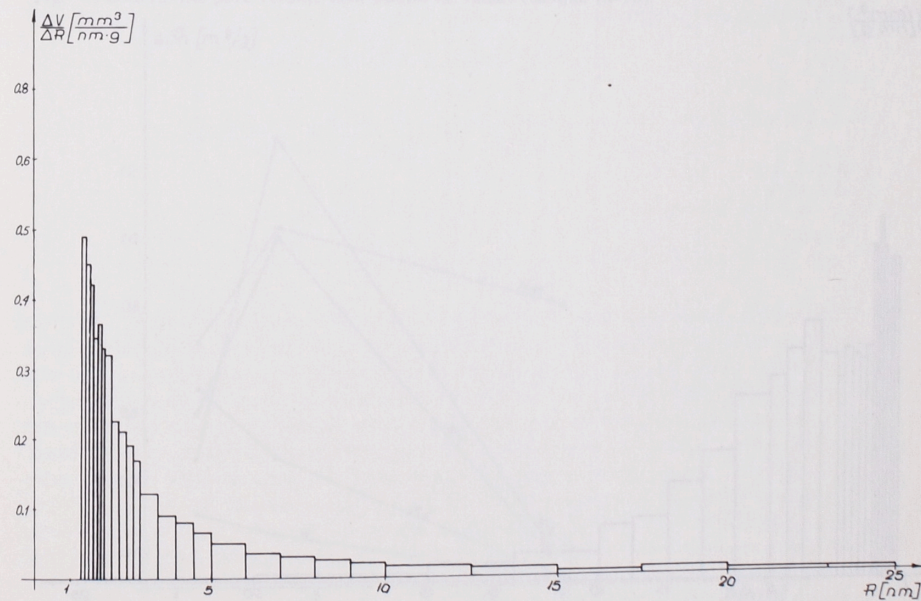


Fig. 4. Differential pore volume distribution vs. radius (sample M-1)

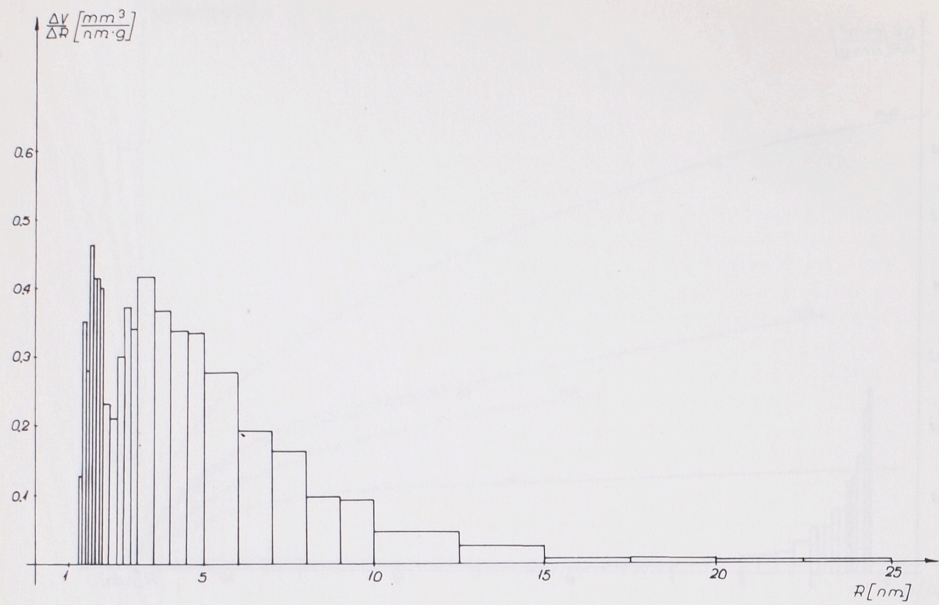


Fig. 5. Differential pore volume distribution vs. radius (sample M-3)

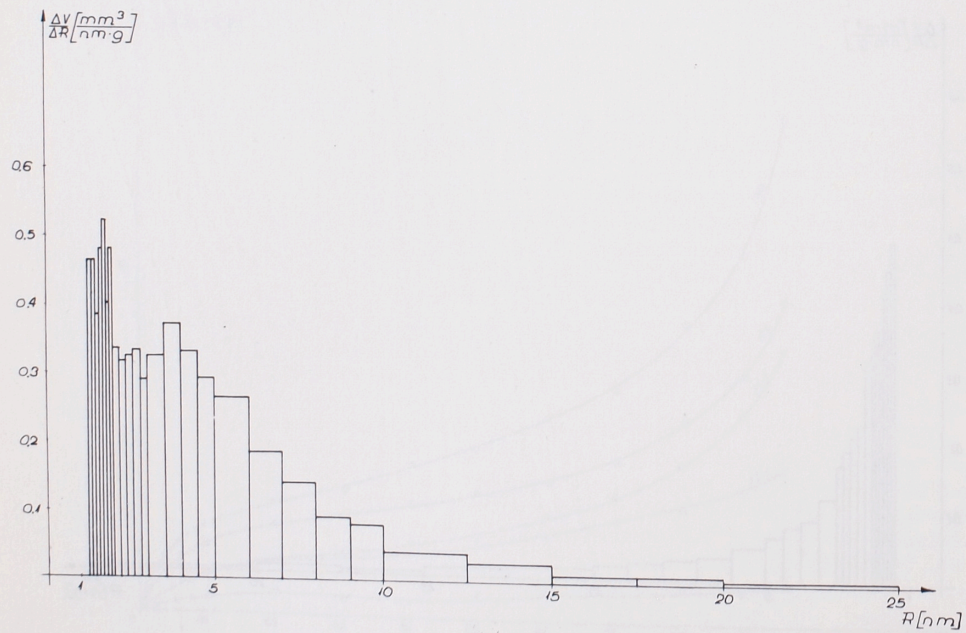


Fig. 6. Differential pore volume distribution vs. radius (sample M-4)

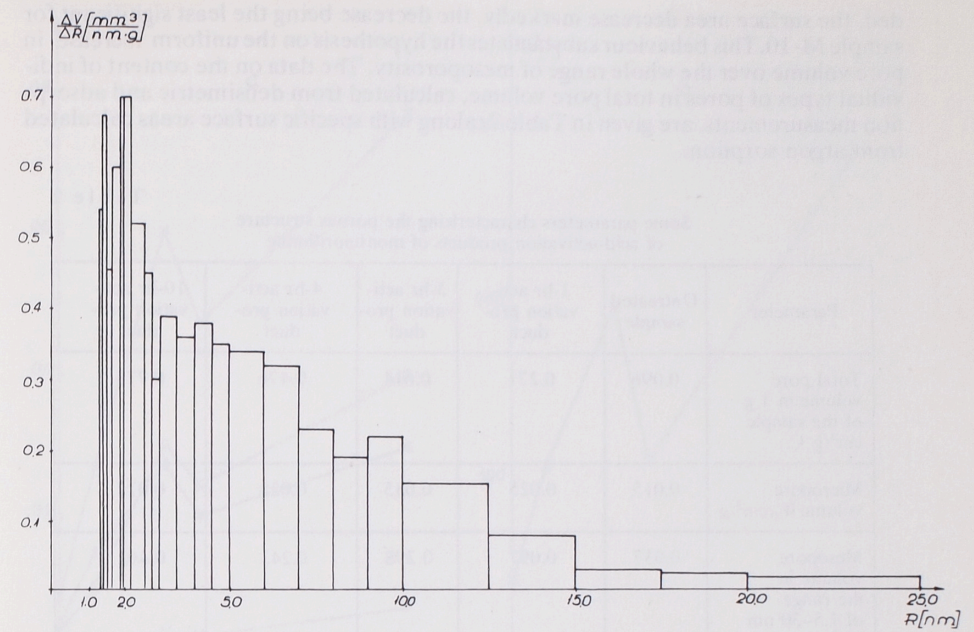


Fig. 7. Differential pore volume distribution vs. radius (sample M-10)

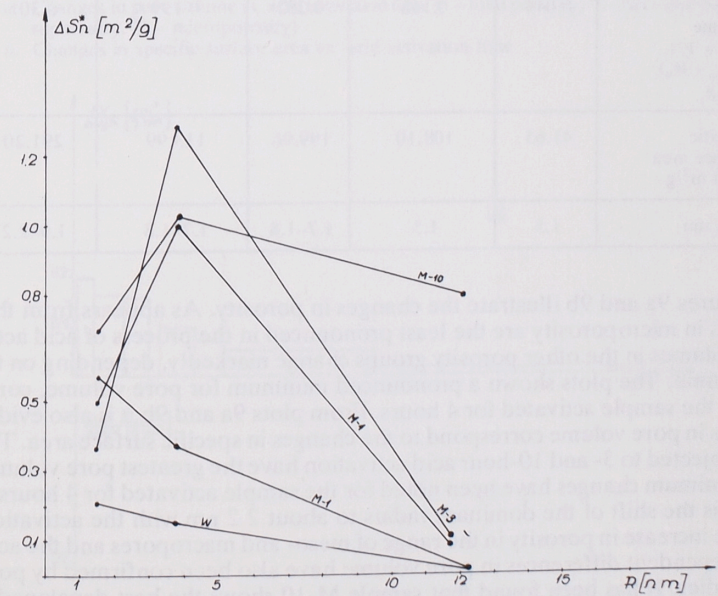


Fig. 8. Plot of radius r vs. mesopore area increase for respective samples

ded, the surface area decrease markedly, the decrease being the least significant for sample M-10. This behaviour substantiates the hypothesis on the uniform increase in pore volume over the whole range of mesoporosity. The data on the content of individual types of pores in total pore volume, calculated from densimetric and adsorption measurements, are given in Table 2, along with specific surface areas calculated from argon sorption.

Table 2
Some parameters characterizing the porous structure of acid-activation products of montmorillonite

Parameter	Untreated sample	1-hr activation product	3-hr activation product	4-hr activation product	10-hr activation product
Total pore volume in 1 g of the sample V_t , cm^3/g	0.096	0.271	0.614	0.476	0.775
Micropore volume W_0 , cm^3/g	0.015	0.025	0.035	0.028	0.072
Mesopore volume in the range of 1.5–30 nm V_m , cm^3/g	0.037	0.097	0.298	0.243	0.402
Macropore volume $V_{mac} = V_t - (V_m + W_0)$, cm^3/g	0.044	0.148	0.282	0.199	0.301
Specific surface area SBET m^2/g	41.65	108.10	199.96	113.99	291.20
r_{dom} , nm	1.5	1.5	1.7–1.8	1.7–1.8	1.9–2.2

Figures 9a and 9b illustrate the changes in porosity. As appears from the plots, changes in microporosity are the least pronounced in the process of acid activation. Pore volumes in the other porosity groups change markedly, depending on the activation time. The plots shown a pronounced minimum for pore volume, corresponding to the sample activated for 4 hours. From plots 9a and 9b it is also evident that changes in pore volume correspond to the changes in specific surface area. The samples subjected to 3- and 10-hour acid activation have the greatest pore volume, whereas minimum changes have been noted for the sample activated for 4 hours. Worth noting is the shift of the dominant radius to about 2.2 nm with the activation time.

The increase in porosity in the range of meso- and macropores and the activation time-dependent differences in pore volume have also been confirmed by porosimetric studies. It has been found that sample M-10 shows the best developed porous structure. In this activation product the dominant pore radius is between 35 and 40 nm. From a comparison of differential pore volume distribution curves it can be

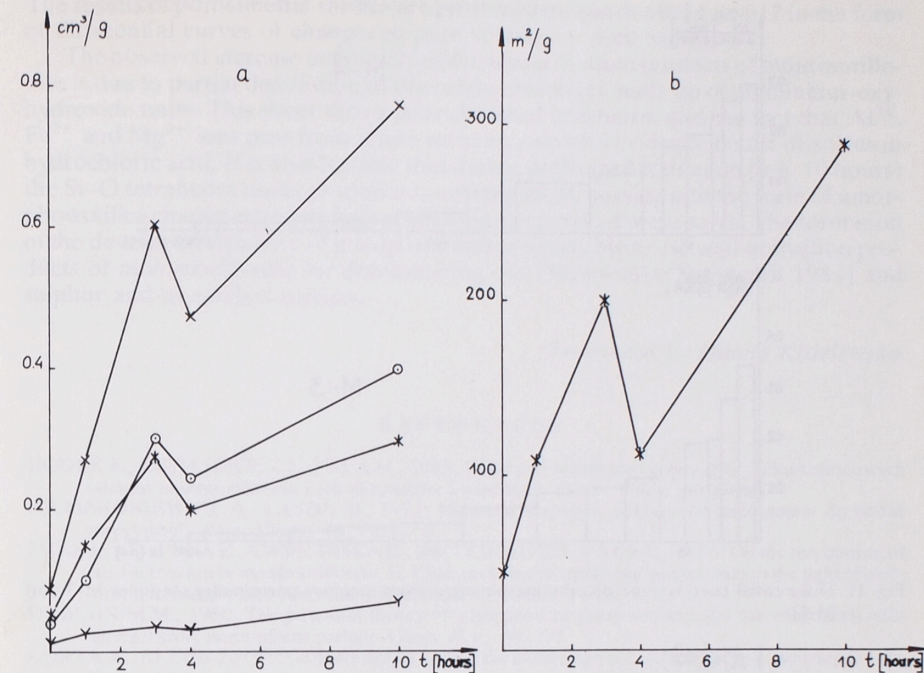


Fig. 9. a. Changes in pore volume vs. acid activation time (x – total porosity, * – macroporosity, o – mesoporosity, y – microporosity)
b. Changes in specific surface area vs. acid activation time

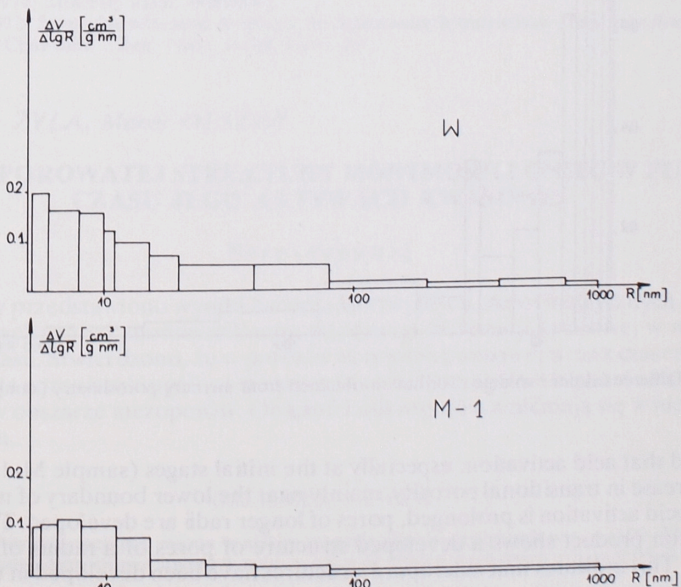


Fig. 10. Differential pore volume distribution obtained from mercury porosimetry (samples W and M-1)

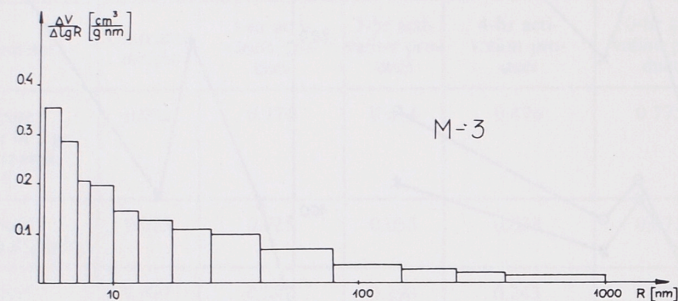
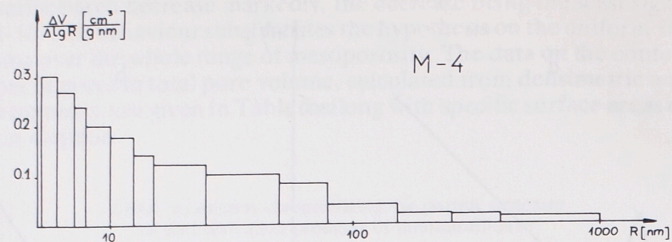


Fig. 11. Differential pore volume distribution obtained from mercury porosimetry (samples M-3 and M-4)

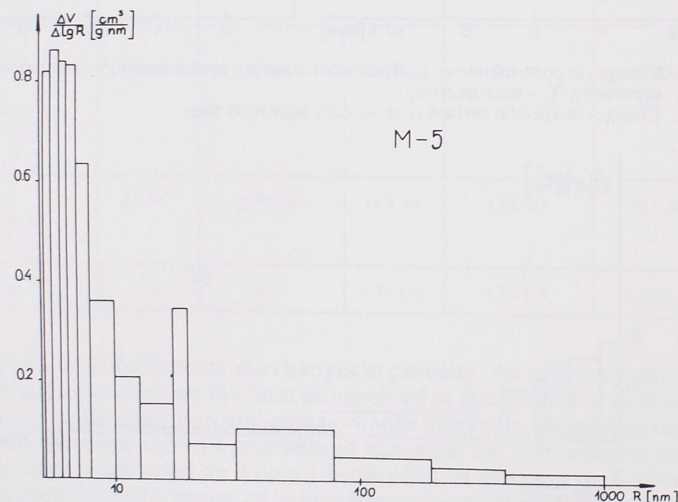


Fig. 12. Differential pore volume distribution obtained from mercury porosimetry (sample M-5)

inferred that acid activation, especially at the initial stages (sample M-1), results in the increase in transitional porosity, mainly near the lower boundary of mesoporosity. As acid activation is prolonged, pores of longer radii are developed. The 10-hour activation product shows a developed structure of pores of a radius of more than 30 nm. This indicates that macropore structures have been developed in this sample.

The results of porosimetric studies are presented in figures 10, 11 and 12 in the form of differential curves of changes in pore volume vs. pore radius r .

The observed increase in porosity of the acid activation products of montmorillonite is due to partial dissolution of the octahedral sheet made up of aluminium-oxyhydroxide units. This sheet shows poor chemical resistance, and the fact that Al^{3+} , Fe^{2+} and Mg^{2+} ions pass from it into solution provides evidence that it dissolves in hydrochloric acid. It is also feasible that during prolonged activation (e.g. 10 hours) the Si-O tetrahedra undergo spatial re-arrangement, passing into the form of amorphous silica characterized by high porosity in the range of mesopores. The formation of the developed structure of mesopores makes it possible to use acid-activation products of montmorillonite for decolourizing oils (Rutkowski, Stajszczyk 1981) and sulphur and as catalyst carriers.

Translated by Hanna Kisielewska

REFERENCES

- BODEK E., ZIĘTKIEWICZ J., ŻYŁA M., 1983; Własności sorpcyjne i porowatość kilku kationowych odmian montmorillonitu i ich aktywatorów kwasowych. *Miner. Polon.* (in press).
- CIEMBRONIEWICZ A., LASON M., 1972; Manostat sorpcyjny półautomatyczny aparat do badań sorpcyjnych. *Rocz. Chem.*, 46, 703-710.
- FIJAŁ J., KŁĄPYTA Z., KWIECIŃSKA B., ZIĘTKIEWICZ J., ŻYŁA M., 1975; On the mechanism of acid activation of montmorillonite. II. Changes in the morphology and porosity in the light of electron microscopic and adsorption investigations. *Miner. Polon.* 6, 2.
- DUBININ M.M., 1960; The potential theory of adsorption of gases and vapours for adsorbents with energetically nonuniform surface. *Chem. Rev.*, 60, 235.
- KORTA A., KLINIK J., 1979; An attempt to specify the evaluation of parameters characterizing the cylindrical mesopore texture from vapour desorption isotherms. *Pol. J. Chem.*, 53, 653.
- NOVAK J., GREGOR M., 1969; Surface and decolorizing ability of some acid-treated montmorillonites. Proceedings of the International Clay Conference. Tokyo, 1, 851-857.
- RUTKOWSKI M., STAJSZCZYK K., 1981; Zdolności odbarwiające a struktura porowata ziem. *Przem.Chem.* 60. (5), 287.
- STOCH L., 1974; *Minerały ilaste*. Warszawa.
- ŻYŁA M., 1972; Sorpcyjne własności termiczne modyfikowanych bentonitów i montmorillonitu z kopalni "Chmielnik". *Zesz. Nauk. AGH, Górn.* 48.

Mieczysław ŻYŁA, Marek OLSZAR

ZMIANA POROWATEJ STRUKTURY MONTMORILLONITU W FUNKCJI CZASU JEGO AKTYWACJI KWASOWEJ

Streszczenie

W pracy przedstawiono wyniki badań adsorpcyjnych, densymetrycznych i porozymetrycznych próbek montmorillonitu poddanego aktywacji kwasowej w różnych okresach czasu. Stwierdzono, że w procesie aktywacji kwasowej wraz z czasem aktywacji wzrasta porowatość ogólna i mezoporowatość. Szczególnie silne zróżnicowanie występuje w obszarze mezoporów. Objętości mikroporów zmieniają się w nieznacznym stopniu.

OBJAŚNIENIA FIGUR

- Fig. 1. Izotermy adsorpcji par argonu w niskim zakresie ciśnień względnych $p/p_0 = 0,00-0,05$
- Fig. 2. Izotermy adsorpcji par argonu w pełnym zakresie ciśnień względnych $p/p_0 = 0,05-0,97$

- Fig. 3. Różniczkowy rozkład objętości porów w funkcji promienia (próbka W)
 Fig. 4. Różniczkowy rozkład objętości porów w funkcji promienia (próbka M-1)
 Fig. 5. Różniczkowy rozkład objętości porów w funkcji promienia (próbka M-3)
 Fig. 6. Różniczkowy rozkład objętości porów w funkcji promienia (próbka M-4)
 Fig. 7. Różniczkowy rozkład objętości porów w funkcji promienia (próbka M-10)
 Fig. 8. Wykres zależności promienia R w funkcji przyrostu powierzchni mezoporów dla poszczególnych próbek
 Fig. 9. a. Zmiana objętości porów w funkcji czasu aktywacji kwasowej (x – porowatość całkowita, * – makroporowatość, \odot – mezoporowatość, Υ – mikroporowatość).
 b. Zmiana powierzchni właściwej w funkcji czasu aktywacji kwasowej.
 Fig. 10. Różniczkowy rozkład objętości porów uzyskany metodą porozymetrii rtęciowej (próbki W i M-1)
 Fig. 11. Różniczkowy rozkład objętości porów uzyskany metodą porozymetrii rtęciowej (próbki M-3 i M-4)
 Fig. 12. Różniczkowy rozkład objętości porów uzyskany metodą porozymetrii rtęciowej (próbka M-5)

Мечислав ЖИЛА, Марек ОЛЬШАР

ИЗМЕНЕНИЕ ПОРИСТОЙ СТРУКТУРЫ МОНТМОРИЛЛОНИТА В ФУНКЦИИ ВРЕМЕНИ ЕГО КИСЛОТНОЙ АКТИВАЦИИ

Резюме

В работе изложены результаты адсорбционных, денсиметрических и порозиметрических исследований проб монтмориллонита, подвергнутого кислотной активации в разных периодах времени. Было отмечено, что в процессе кислотной активации его общая пористость и мезопористость повышается пропорционально времени активации. Особенно сильная дифференциация наблюдается в области мезопор. Объем микропор изменяется в незначительной степени.

ОБЪЯСНЕНИЯ К ФИГУРАМ

- Fig. 1. Изотермы адсорбции паров аргона в диапазоне низких относительных давлений $p/p_0 = 0,00-0,05$
 Fig. 2. Изотермы адсорбции паров аргона в полном диапазоне относительных давлений $p/p_0 = 0,05-0,97$
 Fig. 3. Дифференциальное распределение объема пор в функции радиуса (проба W)
 Fig. 4. Дифференциальное распределение объема пор в функции радиуса (проба M-1)
 Fig. 5. Дифференциальное распределение объема пор в функции радиуса (проба M-3)
 Fig. 6. Дифференциальное распределение объема пор в функции радиуса (проба M-4)
 Fig. 7. Дифференциальное распределение объема пор в функции радиуса (проба M-10)
 Fig. 8. Кривая зависимости радиуса R в функции приращения поверхности мезопор для отдельных проб
 Fig. 9. a. Изменение объема пор в функции времени кислотной активации (x – полная пористость, * – макropористость, \odot – мезопористость, Υ – микропористость)
 b. изменение собственной поверхности в функции времени кислотной активации
 Fig. 10. Дифференциальное распределение объема пор, полученное методом ртутной порозиметрии (пробы W и M-1)
 Fig. 11. Дифференциальное распределение объема пор, полученное методом ртутной порозиметрии (пробы M-3 и M-4)
 Fig. 12. Дифференциальное распределение объема пор, полученное методом ртутной порозиметрии (проба M-5)